Chapter 10

Study of Fracture Mechanisms at Cyclic Fatigue of Austenitic Steels Used in Nuclear Reactors

Tamaz Eterashvili

Additional information is available at the end of the chapter

http://dx.doi.org/10.5772/intechopen.70953

Abstract

The presented work deals with the possible reasons of nucleation and propagation of macro-, meso-, and microcracks after low-cycle fatigue (LCF) tests of stainless, austenitic steels at room temperature. This research will also support the solution of some important problems of steel modeling and their application to EURATOM, FUSION, TACIS, PHARE, CORDIS, PERFECT, AMES, FP 7, and GEN IV programs. The scanning electron microscopic (SEM), X-ray, and transmission electron microscopic (TEM) examinations and statistical analysis of the samples which undergone the low-cycle fatigue (LCF) showed that the average length of slip bands and micro-components of macrocrack are equal, and they are always parallel to each other, indicating their crystallographic character. The microcracks in these samples, caused by the residual stresses after the LCF, were studied in the TEM samples after their preparation to reveal the features of microcrack initiation and nucleation. It was shown that microcracks propagate along slip bands and change their propagation direction at the boundaries of grains and subgrains. This confirms that microcracks, as well as micro-components of mesocrack, are crystallographic. Mathematical calculations of elastic-plastic model are also performed which showed that the length of plastic zone, according to our assessments, is equal to 110–120 d, where d is a width of crack opening.

Keywords: fracture, fatigue, SEM, TEM, slip band, twin, microcrack, microstructure, plastic zone

1. Introduction

Among others, the problem of low-cycle fatigue (LCF) fracture is of particular interest, and a number of papers and monographs are dealing with this problem. It is known that nucleation of microcracks in the austenitic, fine-grained steels was observed in slip bands. In the recent publications, the key role in the destruction of the material is assigned to precipitates and grain

boundaries as well, such as MC-type carbides that precipitate mainly on grain boundaries. It was also shown that nucleation of fatigue cracks occurs at nonmetallic inclusions; however, the trajectory of further propagation of the crack passes through the sites of local stresses with equal magnitudes. The authors of [1] assumed that in stainless steel 304, at different fatigue cycles, size of nucleated crack depends on the intensity of stress. Stress intensity factor (K), to influences the plastic zone size as well, resulting in a complicated dependence of the latter on K [2]. In work [2], it carried out a modeling of plastic zone behavior during a ductile-brittle fatigue and found a certain correlation between the plastic zone size ahead of the arrested crack and the stress intensity factor. Local and global anisotropy considerably affects mechanical behavior of materials, mostly when the dimensions of microcracks and grains are comparable. There are also indications that the cracks of the above dimensions propagate with considerable deviations and more intensively at the initial stage of crack growth. Notwithstanding, this "anomalous behavior" is usually attributed to the crystallography of grains; its reasons are not yet fully understood. The varying orientations of grains may create nonuniform stress field. Generally, the influence of the fields is not taken into account for characterization of fracture process. Usually, the growth of small cracks is described in terms of linear elastic fracture mechanics (LEFM); the considerations of the latter are applicable for large cracks as well. Therefore, the local anisotropy of grain is neglected in Ref. [3], and the influence of local alteration of elasticity modulus on mechanical fracture of "microstructurally small" cracks has been estimated, in particular, of the stress intensity factor (SIF) K and its variation with regard to random crystallographic orientations of grains. The microcrack propagation process and its correlation with the microstructure of the steel are also quite disputable. Despite numerous experimental results on alteration of microcrack propagation direction, there is no convincing hypothesis explaining the real reasons for the process. The main goal of the proposed work is the careful study of the problems described above. For this purpose different grades of chromium austenitic steels have been examined which are the prospective materials for structural parts subjected to extreme cyclic loading and severe environmental conditions.

2. Experimental

2.1. Materials and their treatment

Standard cylindrical samples for cyclic tests were cut off from the thermally treated rods using lath and milling tool. Some of the samples were of square cross section. Working parts of the samples were polished for metallographic analysis. Austenitic grains were revealed by chemical etching. After completion of 20, 30, 40, and 50% of cyclic deformation of fatigue tests, at different amplitudes of deformation, ±0.05 and ±0.5, the evolution of slip lines was studied (**Table 1**). The characterizations were carried out by scanning electron microscope. Fractographic characterizations were carried out after rupture of the samples using a scanning microscope. The local plastic deformation rate and the magnitude of the respective stresses within the micro-area of a grain were determined. The samples for transmission electron microscopic (TEM) investigations were prepared by mechanical polishing and then electrolytic and/or ion bombardment

http://dx.doi.org/10.5772/intechopen.70953

	Content wt%									
Steel grades	**C**	**Si**	**Mn**	**Cr**	**Ni**	**Ti**	**Mo**	**Nb**	**S**	**P**
X18H10T-AISI-321	0.08–0.12	0.7–0.8	1–2	17–19	9–11	0.5–0.7	—	—	0.015–0.02	0.03–0.035
X18H12Б-AISI 347	0.06–0.08	0.8–1.0	1–2	17–19	11–13	—	—	1.0–1.1	0.2–0.025	0.03–0.035

Table 1. Chemical composition (wt%) of the investigated steels.

techniques. In order to reveal the location of stress concentrations, electron beam defocusing was applied. Via stereographic and crystallographic analysis and computer simulation of the respective schemes, the following were determined: the direction of the slip lines, modes of deformation twins, stacking faults, and microcracks. On the basis of the obtained experimental results, some possible theoretical models of microcrack initiation mechanisms have been considered. The above heat treatments lead to the formation of big austenitic grains that supported the study of plastic processes taking place within one austenitic grain.

2.2. Low-cycle fatigue (LCF) tests

LCF tests were performed at room temperature. Two regimes were used: (1) The same amplitude of deformation ±0.05 mm and different frequencies of cycling, 0.33 and 0.45 Hz, and (2) frequency, 0.45 Hz, and amplitudes ±0.05 and ±0.1 mm. The cylindrical samples were loaded cyclically with the magnitude of loading 100–3000 kg. For scanning electron microscopic (SEM) study, in some cases, the V-notched plate-like samples were also used. All samples were subjected to continuous cyclic loading.

3. Results

3.1. Scanning electron microscopic (SEM) investigations

The SEM study of the samples revealed a peculiar polycrystalline structure of austenite. The sizes of austenite grains vary from 30 to 70 μm, depending on grade and treatment of the steel. In some large austenite grains, the recrystallization twins and variety of shapes of grains were also observed. The grains turn rounded; acute angles and joints between the grains become smoother. The majority of the metallographic sections showed the austenite grains with the diameters of 30–70 μm. After cycling (n = 2000), a macrocrack was formed on the metallographic section, and a 150–250 μm width zone with the plastic features was also detected at the tip and the both sides of the macrocrack. After subsequent fatigue tests, the width of the zone increased up to 250–300 μm. Within the plastic zone, in addition to the heavily deformed grains, some partially deformed or even non-deformed grains were revealed. As a rule, they were formed at the boundaries of the large grains and twins and at joints of grains. In addition to the localized slip bands in the plastic zone of some grains, an intensive plastic flow was detected in the form of parallel slip bands covering the part of the grain.

Further cyclic fatigue deformation, in addition to the existing slip bands, caused the creation of some new ones (**Figures 1** and **2**). The variation of lengths of the slip bands and the respective statistical curves (**Figure 3**(n_1)) revealed that most of the bands are of 10–30 μm length. Further tests lead to the formation of the additional slip bands that, in contrast to the previous ones, are shorter and less neat, while their maximal number remains the same (**Figure 3**(n_2)). Further fatigue tests caused a minor (20%) increase in the lengths of the slip bands. The widths of the bands increased 2–3 times. However, in spite of the latter, the slip bands do not cover the whole width of the austenite grain. The measurements of angles between the axis of loading and the slip bands showed that the first slip bands are oriented at an angle of 30–70°. However, the majority of slip bands were formed along the direction of maximal tangent stresses (45°). The direction of the slip bands, formed at later stages of the test, nearly or completely coincides with the direction of the macrocrack propagation.

3.2. Macrocracks

As it was noted above, at the crack tip and around it, the slip bands and isolated mesocracks were observed. Most frequently, the isolated mesocracks were formed near the slip bands. However, in some cases, they were observed inside small grains as well. It should be noted particularly that deformation in plastic zone flows rather heterogeneously. In the places of deviation, a plastic deformation takes place in the form of slip bands (**Figures 2** and **4**). The macrocrack consists of individual micro-components.

In the 30–50 μm area near the crack tip, a plastic deformation of a higher rate than at both sides of the crack was detected. The latter is exhibited in the form of the enhanced homogeneous slip in the surface plain of the sample and in the direction perpendicular to it, and the localized slip bands become coarser. The variation of the lengths of micro-components of the macrocrack showed that after n_2 = 4000 cycles their lengths vary between 10 and 30 μm. However,

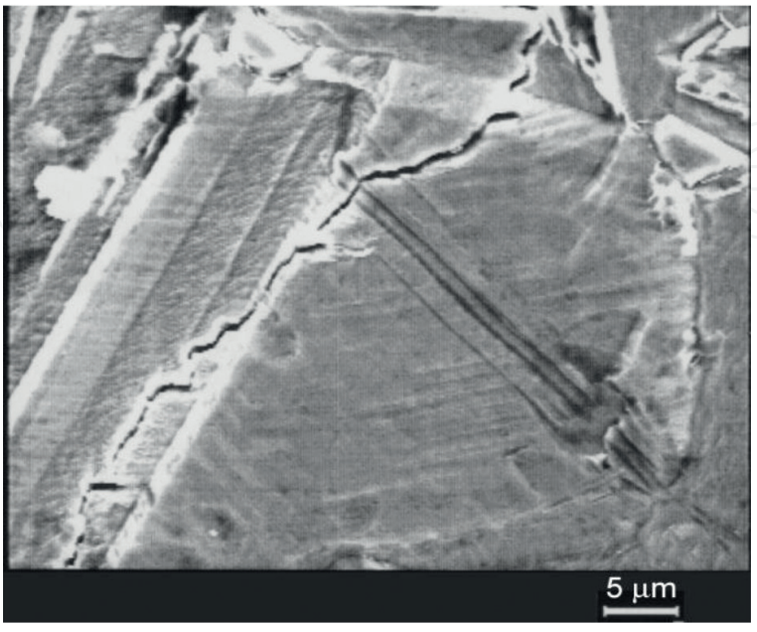

Figure 1. Localized slip bands near the large carbides and other inclusions (X18H10T mode II).

http://dx.doi.org/10.5772/intechopen.70953

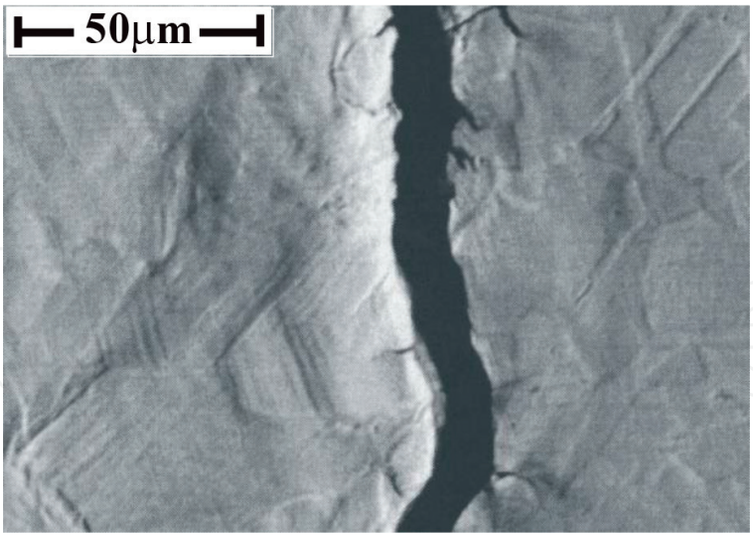

Figure 2. Intensive plastic flow, near a macrocrack in the steel X18H12Б (mode I). (SEM image).

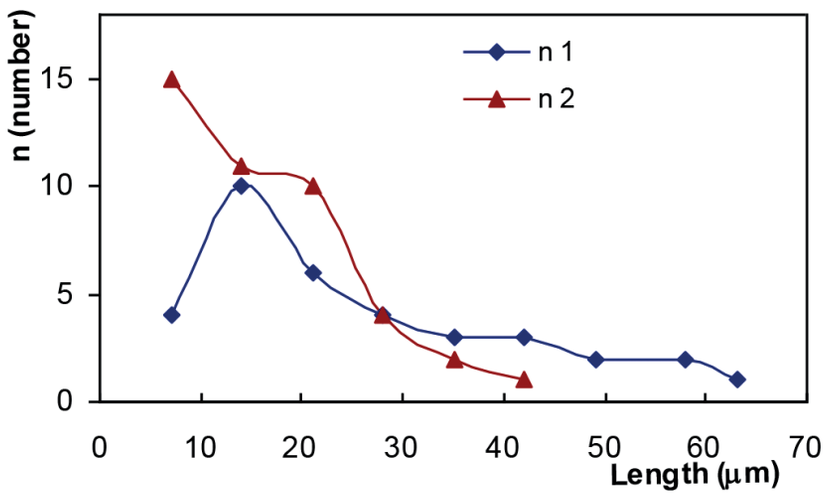

Figure 3. Statistical distribution of the lengths of slip bands (n_1 = 2000 and n_2 = 4000 (X18H12Б)).

the lengths of the micro-components decrease after subsequent tests. The angles of deviation of the micro-components from the axis of cycling were also measured. As it is evident, the majority of micro-components deviate at an angle of 80–90°. The macrocrack passes through the twin/matrix boundaries without any significant deviations as well. It was also revealed that the dimensions of micro-components of a macrocrack and microstructure elements of the steel better coincide in the lower range of lengths. Thus, in the growth and propagation, the macrocrack correlates with the microstructure elements of the steel. Thus, one may assume that micro-components of macrocrack are influenced by the crystallography of the material.

3.3. Isolated mesocracks

In plastic zone, some individual, isolated mesocracks were also detected in addition to the slip bands (**Figure 4**). They mainly nucleate at (or on) the grain boundaries with no apparent signs

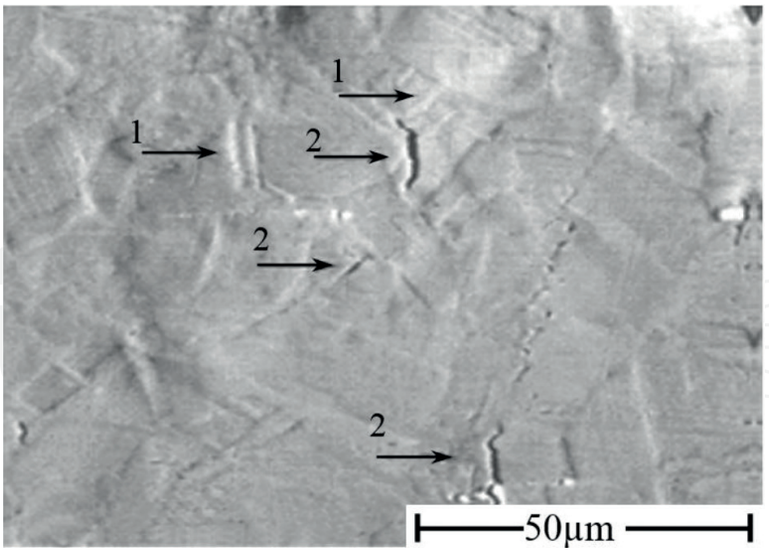

Figure 4. Plastic zone ahead of the fatigue macrocrack ((1) slip bands, (2) microcracks).

of plastic deformation (e.g., slip bands), while the isolated mesocracks were quite frequently observed within the small grains as well. In some areas, they are grouped, while in the others, the distance between them is 50–60 μm. As the isolated mesocracks are located in the plastic zone, the distance between the macrocrack and the utmost mesocrack is controlled by the dimensions of a plastic zone (250–350 μm). Here, we also have to note the experimentally observed fact that the directions of the isolated mesocracks and the slip bands often (but not always) coincide. In the grains in which the isolated mesocracks were formed, no localized slip bands were observed. Thus, it should be supposed that the mesocracks were formed near the border of plastic zone. In the majority of cases, the orientation of mesocrack coincides or is close to the main direction of macrocrack [4]. Analysis of different areas of the zone and measurements showed that the size of the plastic zone is related to that of macrocrack, and an increase in macrocrack size increases plastic zone size. The maximal size of plastic zone ahead of macrocrack tip detected in our experiments was equal to 250–350 μm (**Figure 4**).

The macrocrack is localized in a narrow zone 600 μm wide in which isolated meso- and microcracks and slip bands are observed. Clearly, the size varies depending on chemical composition and heat treatment of the steel; however, the correlation between macrocrack size and the plastic zone size still exists. The shape of the plastic zone is close to a spherical or compressed ellipse. Theoretical solution of this problem is foreseen in the proposed project based on an elastic-plastic model using the linear theory of elasticity.

3.4. The elastic-plastic model

The simple assumption on fatigue failure mechanism in the conditions of plain strain leads to the formation of a small plastically deformed volume ahead of microcrack, called the crack tip plastic zone. The zone is cylindrical with the radius R and the axis is oriented as shown in **Figure 5**. If the radius (R) of the relaxation zone is less than the crack length (L), the stress in the middle of the crack practically will not be affected by the plastic relaxation.

http://dx.doi.org/10.5772/intechopen.70953

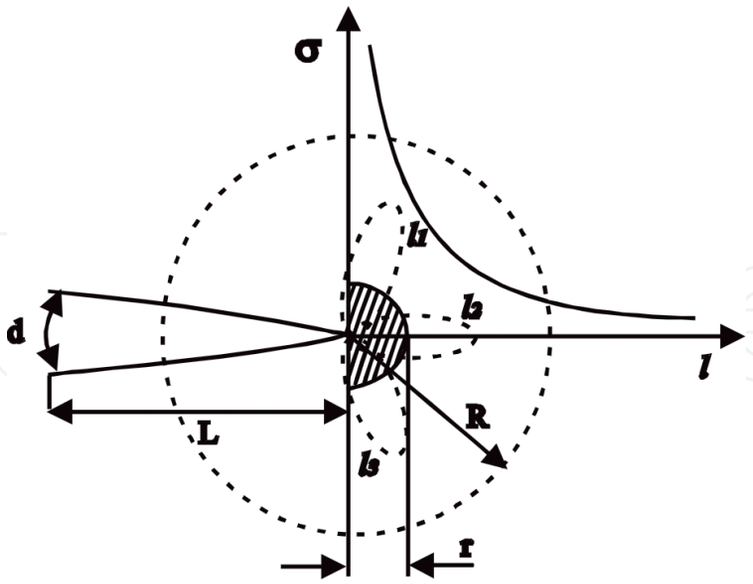

Figure 5. Theoretical scheme, of the cylindrical plastic zone, ahead of the crack tip. Here, *r* s a radius of destruction zone, and l_1, l_2, and l_3 are dimensions of different plastic characteristics (slip bands, twins, and microcracks).

In addition, the crack width (d) remains the same. Our experiments show that the edges of the cracks near the crack tip are parallel to each other. According to the linear elastic fracture mechanics, the magnitude of the stress applied perpendicularly to the microcrack growth direction in the vicinity of a crack tip is of the form

$$\sigma_F^2 = K^2/2\pi R \tag{1}$$

In order to evaluate the size of the plastic zone, let us suppose that on the interface between the plastic and elastic zones the magnitude of stress (σ_E) is equal to the yield strength of the material (σ_F). However, based on the above supposition, we are considering only the interface between plastic and elastic zones. Here, it should be noted that the formula contains a stress intensity factor (K), being quite difficult to determine

$$R = \frac{K^2}{2\pi\sigma_F^2} \tag{2}$$

unambiguously (in addition to the stressed state, the factor K depends on the shape of the microcrack as well). In the present work, an attempt is made to exclude this factor from Eq. (2). To characterize the material resistance to crack propagation, a critical value of crack opening (d) may be used instead of K. According to the reported results of a number of authors, this value may be used in the cases of substantial plastic deformations as well. When the material with several slip systems (in our case of FCC crystal it has) is analyzed, the elastic stresses occurred near the crack tip are almost completely relaxed in the plastic zone, while in the elastic zone, they still exist, and K characterizes the stressed state. As a result, the crack tip turns blunt, and the edges go parallel to each other, except the area at the very tip. In plastic zone, the dislocations are in equilibrium state because of yield stress (σ_F) and the external stress (σ) applied from the side of the microcrack:

$$I = \mathrm{nb}\sigma_F \tag{3}$$

Here, I is a Rice integral [5] which determines the energy flow to the crack tip or the body potential energy change after the crack length is varied. Especially, I determines a free energy per unit length of the crack ($I = -\partial w/\partial h$). In the cases when $R \ll L$, that is, for small plastic zones, we arrive at the following expression for the planar stressed state:

$$I = K^2/E \tag{4}$$

Here, E is a Young modulus. However, as it follows from Rice integral, I determines the energy dissipated in the process of crack propagation and is related to the crack opening (d):

$$d = I/\sigma_F \tag{5}$$

$$I = \mathrm{d}\sigma_F \tag{6}$$

The formulae (4) and (6) lead to the exclusion of I, and we arrive at the following formula for K:

$$K^2 = \mathrm{dE}\sigma_F \tag{7}$$

From Eqs. (7) and (2), we will also have for R

$$R = \frac{\mathrm{dE}}{2\pi\sigma_F} \tag{8}$$

Thus, the plastic zone size can be determined this way, knowing E and σ_F of the material. Calculations of R for the steel with E = 195,000 MPa and σ_F = 280 MPa showed that for this steel $R \cong 110\ d$, that is, it is equal to 300–350 μm that coincides with our experimental measurements ($r \cong 0.1\ R$) [6].

4. TEM examination structure changes after LCF

As it was shown above, the size of the plastic zone ahead of macrocrack amounts to 250–300 μ (spherical or ellipsoid). For TEM studies we used samples with the diameter of 3 mm and initial thickness 200–250 μ, which subsequently were mechanically ground to 200–250 μ and then electrochemically polished to 500–600 Å. Comparison of this dimension with those of the plastic zones makes it clear that we are not able to study the processes taking place ahead of macrocrack. This means that all the processes in plastic zone can be detected and studied except formation of meso- and microcracks, due to the dissolution of areas adjacent to microcrack during the electrochemical polishing. On the other hand, so big tension is concentrated just ahead of microcrack that during thinning the sample is destructed. However, internal

http://dx.doi.org/10.5772/intechopen.70953

tensions still remain in some areas of the prepared thin film, and after relaxation, they can be revealed in the places of peak tension. For example, in such places it may form structure defects including nanocracks and microcracks. To understand the latter, one should take into consideration that all kinds of fracture, brittle, ductile, and fatigue, flow via dislocation movement that provides formation of slip bands, stacking faults, and deformation twins. Thus, the reason for the formation of the above defects is microflow. In the cases when the microflow is impossible because of sufficient tension, and when the possibility of formation of the above defects is exhausted, a microcrack is nucleated. Subsequently, peak tensions relax in the places of microcrack formation. That is why TEM samples were held for 0.5–1.0 hours at room temperature for redistribution of internal tensions and formation of microcracks and only after that they were examined in the TEM. The stacking faults, traces of dislocation movement, and sometimes even slip bands are also present in addition to twins. The trace and stereographic analysis showed that in all the investigated cases the slip is realized in {111} planes along <110> directions. The microstructure of the steel is substantially changed, and the characteristic polygonal structure of austenite occurs. In the beginning the polygon boundaries are thin and then gradually thicken when deformation increases. The sizes of the polygons vary from 1 to 20 μm. The average orientations of their elongations coincide with the slip direction (<110>). However, disorientation between the polygons is easily observed which ranges from 2 to 4°. The same is with azimuthal disorientation during cyclic deformation. The polygons also differ from each other by the dislocation density and are detected only at polygon boundaries. Further study of fatigue plastic deformation of the investigated steels showed that increase in a number of cycles causes intensive structural transformations in them. The trace and diffraction analysis showed that the slip takes place along the common planes and directions for austenite ({111} and <110>) (**Figure 7**). In addition to the slip bands in some particular grains, a formation of cellular dislocation structure begins (**Figure 8**). At these stages, a dimension of some carbide precipitates decrease. Here should be noted that according to the internal structure of the steel (**Figures 7–9** and **11–13**), in addition to the regular spots, diffuse intensities occur as well (**Figure 9b**). The firstly formed dislocation cells are larger; their dimensions vary from 0.02 to 0.25 μm. The dimensions of dislocation cells gradually decrease after consequent deformations reaching 0.01 μm and, consequently, transform into dislocation balls (**Figure 8**). In some areas, dislocation bundles are formed in which particular dislocations cannot be distinguished. On the one hand, it facilitates the strengthening of the material, and on the other hand, it indicates at enabling other systems of stress relaxation. Along the formation of cells, the process of deformation twinning is going on. Thus, while in one grain, bundles are observed, and in others deformation twins may be observed. Each microstructure element deforms according to its crystallographic orientation to the applied stresses. In the twins as well as in the areas between them, a sufficiently high density of dislocation remains just after the area is completely covered by twins which are almost uniformly distributed within the grain. However, later, an increase of deformation rate increases the density of twins. Further increase of deformation rate provides formation of additional twins angularly with respect to the initial ones, that is, other twin modes come to action. Therefore, in some grains only one mode is detected, while in others two or three different twinning modes are operative. Obviously, just this twinning mode is most probable, and one may suppose that another twinning system comes to action after strengthening of an active one. Thus, twinning provides relaxation of tensions. After the formation of

twins in the majority of grains is over, their size reduction takes place, and thereby the process of fragmentation of the structural elements of the steel starts. Along the directions <110> and <112> (directions of slip and twinning), azimuthal disorientation approaches 20^0 and more. This makes diffraction pattern complicated, and its indexing is ambiguous. In addition, on the diffraction patterns, the extra reflections caused by twins and carbide precipitates appear. At this stage nucleation of martensitic phase takes place, and the respective diffraction spots emerge (**Figure 10**). As the martensitic phase nucleates in deformed austenite, the shape of martensite crystals are the same as of deformation twins. Moreover, they are aligned along the twin propagation direction. To reveal them a the dark-field technique was used which showed that the lengths of martensite crystals are comparable with those of twins. Their lengths are limited by deformation twins and other martensite crystals. The latter becomes apparent through further fining of martensite and deformation twin crystals. The martensite crystals in metastable austenitic phase formed during deformation. The habit pole of the martensitic crystals is situated near the pole of deformation martensite.

5. Characterization of destruction zone ahead of microcrack

5.1. Interaction of microcracks with subgrains

As it was mentioned above, the TEM studies after low-cycle fatigue tests in the TEM samples showed that microcracks are formed in the places of stress concentration and the nucleated microcracks are of different sizes. Sometimes, the main microcrack stops growth along the initial direction, and branching occurs. As our researches have shown, it takes place in the cases when (1) its size is ~5 μm and more and (2) the microcrack rests at an obstacle. The next grains, twins, or subgrains can be such obstacles. Electron diffraction, dark field, trace, and stereographic analyses were used. In **Figure 11(a)** micrograph of one interesting microcrack tip area, with the characteristic defects, is shown. As it is apparent from the electron micrograph, the maim microcrack growth along an initial direction is stopped. Ahead of the microcrack in destruction zone, some defects are present. Let us consider them separately.

5.1.1. The main microcrack

TEM study shows that the main microcrack has long, parallel edges along the <62^{-}4 > direction detected in the zone axis [130]. One may suppose that ahead of the crack tip a relaxation of stress occurs that causes the microcrack arrest. However, the relaxation passed through the formation of defects of another type.

5.1.1.1. Disorientation zone

The zone is characterized by dislocation structure, and the respective diffraction pattern corresponds to [130] zone axis. Its area is equal to 15 μm^2, the central part of which is surrounded by peripheral areas. Crystallographic measurements show that the disorientation between the central and peripheral parts reaches 15–16° and both have almost the same dislocation

http://dx.doi.org/10.5772/intechopen.70953

density. In the central part of the disorientation zone, some prolonged dislocations are observed, parallel to the main microcrack. In addition to the above dislocations, some dislocations, angularly oriented to the microcrack, are also observed in the peripheral parts.

5.1.2. Deformation twins

Two parallel twins with the distance between them 0.4 μm are observed in the direction of the microcrack (**Figure 11(b)**, zone axis [130]: upper (a) and lower (b)). The upper twin is two times larger than the lower. The plane of twinning for both twins is ($1^{-}1^{-}1$), and the direction of the trace is [$62^{-}4$]. The zone axis of the respective electron diffraction pattern is [$51^{-}8$].

5.1.2.1. Arch-like extinction contour

The detected contour is situated nearly in front of the main microcrack along the microcrack growth direction, between the twins 3 and 5. The contour does not contain the lines of dislocation outcrop. In addition, a dislocation cellular structure is revealed, having the archlike shape in this particular case that may be caused by some non-compensated elastic stresses in the contour. Tilting of the sample causes their widening and narrowing near the tip of the microcrack. Thus, the contours serve as in direct signs of the internal stress localization. However, if such case is observed, the curvature of the contours decreases, and short slip bands and dislocation outcrops are detected.

5.1.2.2. Thin twins

Twins with the twin plane (1 1 $^{-}$1), direction of trace <$6^{-}2$ 8>, matrix zone axis [123], and twin zone axis [11^{-} 2. 1^{-}].

5.1.3. Short microcrack

The microcrack is oriented at an angle 37° to the main mesocrack and is almost parallel to the thin deformation twins (5). Here, it should be noted that the angle 37° is the angle between the directions <6^{-}28 > and <$62^{-}4^{-}$ > and the short microcrack is almost parallel to the deformation twins (5), that is, to the direction <6^{-}28>, while the deviation between them amounts to ~5°. The obtained results confirm that in the FCC structures the planes of cleavage, twinning, and slip are the same, while the fracture direction is {111} and is deviated from the twinning shear direction <111> by 6.6°. The above consideration and the analysis of micrographs lead to a conclusion that the destruction zone ahead of the crack tip is confined by the defects (2–6) and these defects practically compose a boundary of the plastic zone. One of the important reasons of steel fracture is a reduction in their relaxation ability during plastic loading. Generally, fracture as well as slip, twinning, fragmentation, disorientation, etc. are the relaxation processes. The fracture (or microcrack propagation) takes place at high stresses, and it is realized after all the above processes are exhausted. Moreover, at high stresses, some processes may flow simultaneously, taking into account the crystallography and Schmidt factor. In the process of stress relaxation in steels, the dislocations will slide along the crystallographic directions (along the planes of slip or twinning) [7].

5.2. Crystallography of the microcracks

Slip bands of different lengths formed near microcracks. The microcracks with long, parallel edges are mainly found inside grains. They are quite long (10–15 μm) and pass through some subgrains, reaching in particular cases the size of some grain diameters. Propagation direction may change within the grain as well while crossing some obstacle such as subgrain boundaries, twins, and carbide precipitates. In addition, to slip bands, near microcracks, stacking faults and dislocation traces are also observed. As it is obvious from the micrographs (**Figure 12**), the microcracks, slip bands, and dislocation traces have the same direction. Moreover, the microcrack propagation direction and the slip bands are always parallel (**Figure 12**). The corresponding diffraction pattern taken from this micro-area shows two FCC zone axes [111] and [114] present simultaneously. The respective stereographic projections show that in the area with the orientation [111] the direction of microcrack propagation is parallel to the slip band. Here, the gnomostereographic projection of the plane (111) is situated in the center of the projection. The microcrack propagation direction and the slip band, in the area with the orientation [114], remain parallel. However, in this case, the normal to the plane of the foil does not lie in the center of the stereographic projection, and consequently the width of the microcrack from the micrograph seems narrower than its real value.

Consequently, the widths of the microcracks in different parts of the subgrain differ. This difference may be derived from the angle between the planes (111) [111] and (11^{-}1) [114]. The results of the calculations are in accordance with those measured experimentally in the micrograph. The performed analyses (statistical, stereographic, and trace) show that the plane of fracture is {111} and the microcrack propagation direction is <110>, in all the considered cases (**Figure 12**). The microcrack propagation direction within subgrain does not vary; however, it changes when passing from one subgrain to another. Thus, the propagation direction is parallel to <110>. The slip bands and stacking faults as well, are oriented along the same directions. This first of all was exhibited in the dislocation structure of the steel. In other words, the stress relaxation occurs just through the formation of these defects. As it was shown by TEM studies, stacking faults, slip bands, and microcracks of two or three different directions were revealed in some grains. The microdiffraction studies and trace analyses showed that the slip occurs along the slip system characteristic of the FCC structure: on {111} planes along the directions <110>. **Figure 12** displays microcracks besides slip bands which are arranged along the slip bands. The microscopic cracks almost always are comparable with the slip bands, both in length and in directions. The boundaries of the micro-area seen in both slip bands and microcracks of three different directions are shown in **Figure 13**. The internal stresses were distributed in the sample and how they relaxed. The trace analysis and microdiffraction studies showed that the direction of propagation of microcracks is <110>. This directly indicates that the microcracks are initiated either in the slip bands or (on) along [8].

5.3. Interaction between microcracks and slip band

As follows from the experimental observations, in practice, only two cases are observed upon the interaction of microcracks with a slip band: when a microcrack propagates in

http://dx.doi.org/10.5772/intechopen.70953

the slip band and when the microcrack is extended at an angle to the slip band. In the first case, the growth of the microcrack will continue until the entire stored energy is spent for its growth or until the microcrack encounters some obstacle after which the microcrack stops. Naturally, during the growth of the microcrack, the possibility of its encounter with another slip bands is not excluded, depending on the level of the accumulated energy. The microcrack will either stop growing along the initial direction or propagate along the direction of the encountered slip band (direction of propagation), or, finally, upon the intersection with the encountered (intersecting) slip band, it initiates a new microcrack into this band, while itself will continue growing along the initial direction of propagation (**Figures 6–13**) [8, 9].

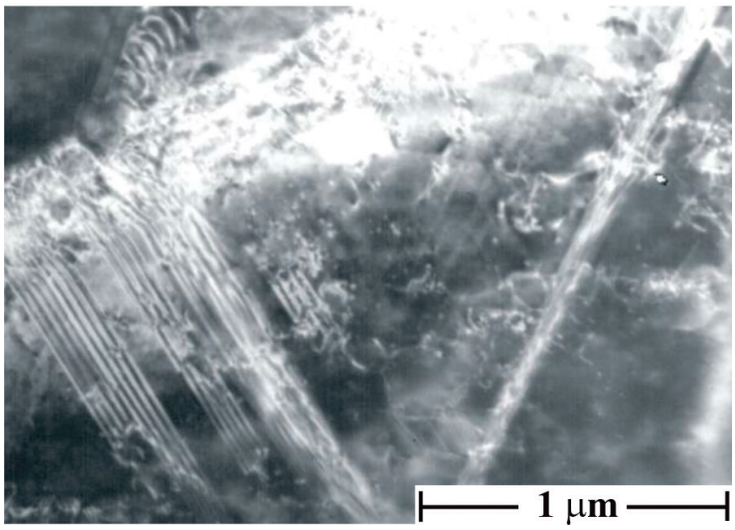

Figure 6. Slip bands and stacking faults. Steel X18 H10T is seen in the upper left part of the micrograph dislocations.

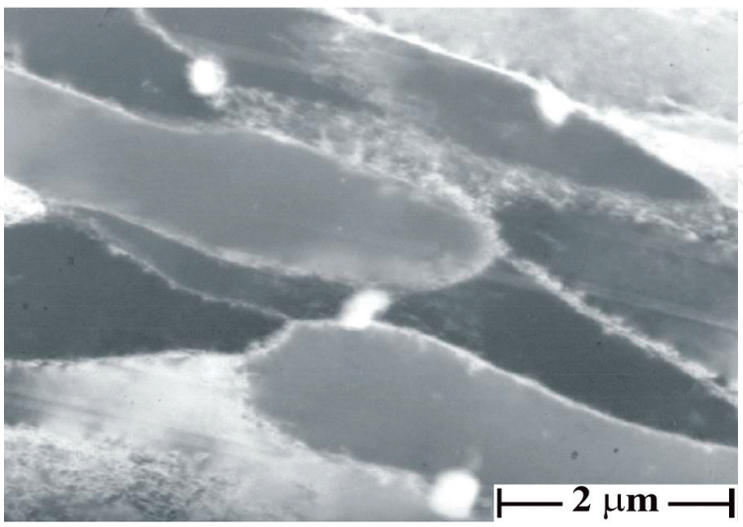

Figure 7. Polygonal structure of the steel after fatigue tests (on the grains of polygons, some carbide precipitates are seen). Direction of polygonization, <110>, steel X18H12Б.

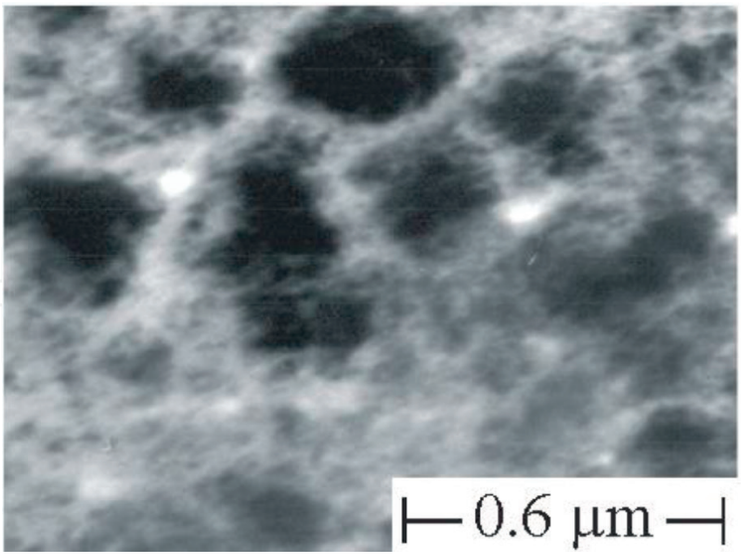

Figure 8. A cellular dislocation structure of the deformed austenitic steel X18H12Б.

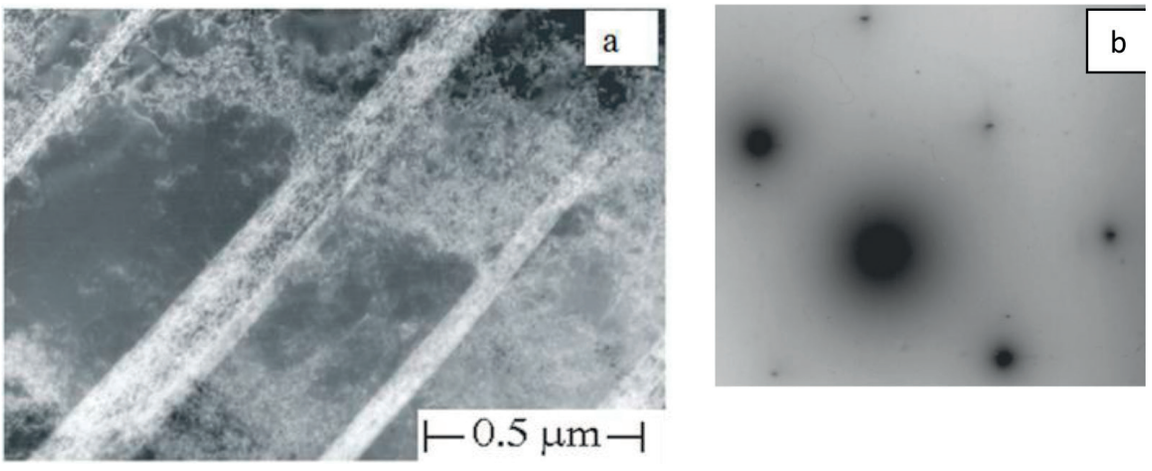

Figure 9. (a) Deformation twins. (b) Zone axis of the matrix [001] is parallel to the zone axis of the twin [221^{-}] (steel X18 H10T).

5.4. Interaction of microcracks with another microcrack

Upon the interaction of a microcrack with another microcrack also, two situations were observed. First, the microcracks propagate along <110> directions as in the same slip band as well as in the adjacent parallel slip bands. In both cases, depending on the level of the stored energy, they can coalesce or stop at a specific distance from each other. However, in some cases, in order to coalesce, they must cause splitting of the area that is located between the microcracks but for this high stresses are required. We did not observe the coalescence of microcracks in this case. In the second situation, when microcracks propagate toward each other at an angle, they almost always unite. In our cases, they stop at small distances from each other. It is likely that in such cases the internal stresses accumulated in the plastic zone are insufficient for the microcracks could continue growing and become coalesced. After the coalescence, the growth continues in

http://dx.doi.org/10.5772/intechopen.70953

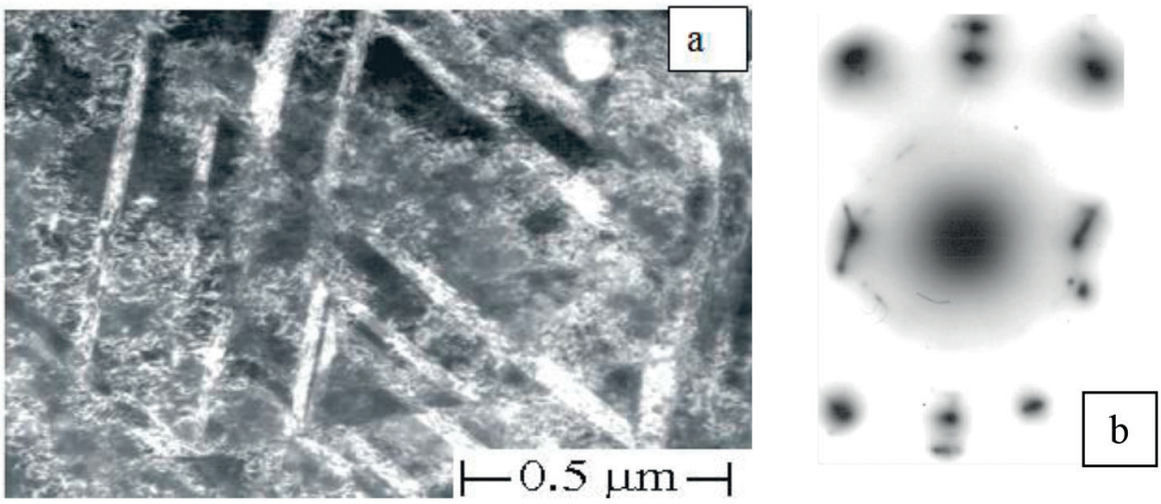

Figure 10. (a) Twins and martensite crystals in the deformed austenite. (b) Zone axis [130] from austenite and reflection (110) from martensite.

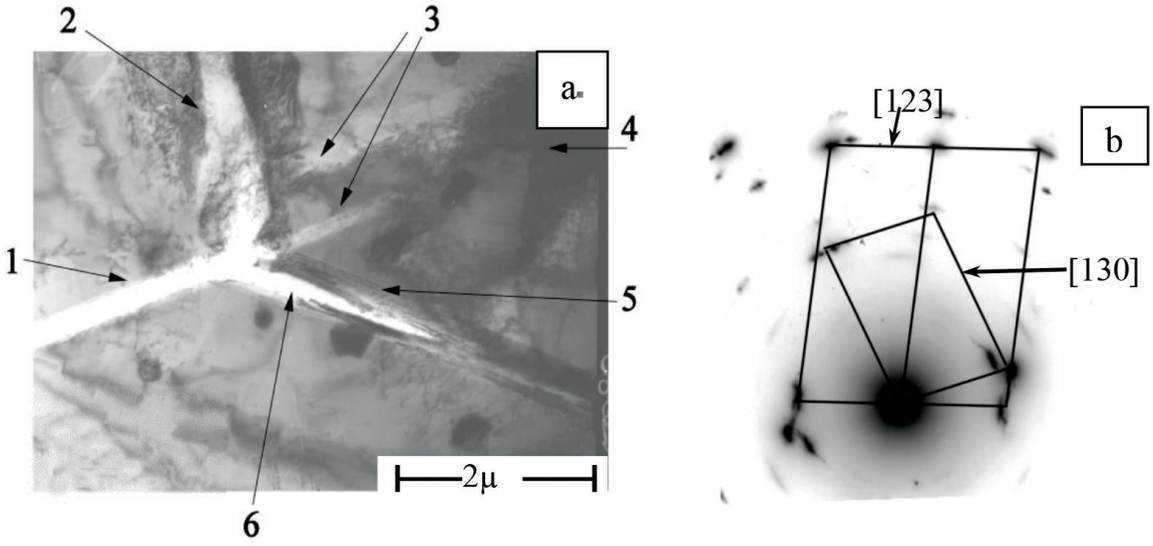

Figure 11. (a) Destruction zone in Cr-Ni-Nb steel. The main microcrack (1); disorientation zone (2); two twins (1) of the direction of microcrack propagation (3); the archlike extinction contour (4); thin twins (5); short microcrack, deviated from the main microcrack but parallel to the twins (6). (b) The indexed electron diffraction pattern, showing traces of twins and microcracks. The scheme is oriented with regard the micrograph.

the direction of one of the microcracks (**Figure 13**). In all the cases examined, it is implied that the direction of the propagation of microcracks remains a crystallographic direction <110>.

5.5. Interaction of a microcrack with carbide inclusions

As it is evident from **Figure 13**, carbide precipitates are also observed in the steel structure together with slip bands and microcracks. In many works it is considered that these are precisely the inclusions of the stress concentrators which are the stacking faults, slip bands, and

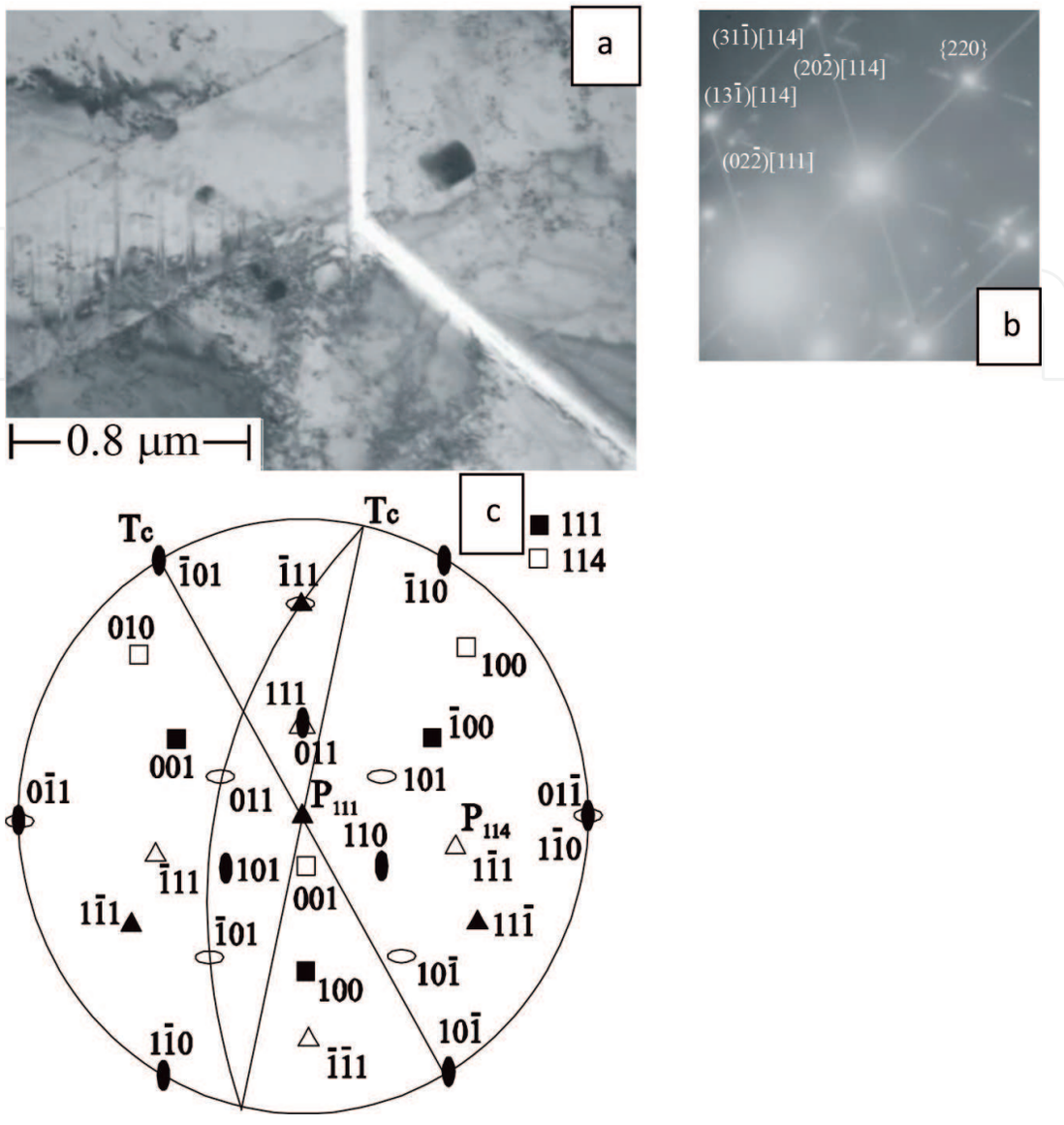

Figure 12. Alteration of microcrack propagation direction at subgrain boundaries, within a grain. (a) A bright-field image of microcrack propagation trajectory (negative image). (b) Electron diffraction pattern. Zone axes [111] (dashed line) and [114] coincide. (c) Stereographic projection.

microcracks in a Cr-Ni-Nb austenitic steel. The electron micrographs show that this is not the case. It is well seen that the inclusions are surrounded by a dislocation tangle (**Figure 13**) and that the dislocation bands ("torches") go out from the region where several inclusions are concentrated. Based on the micrograph, it can be stated that in this specific case the group of inclusions is a barrier to the growth of the microcrack. This follows from the existence of the microcrack whose sharp end rests against the carbide inclusion and the "torches" of stresses are seen apposite to it, which clearly emerge from the tip of the microcrack. They are most likely to be the consequence of the relaxation of stresses that existed before the microcrack tip. Of course, sometimes an opposite picture can be seen, that is, a microcrack that emerges from an inclusion, but this does not make it possible to draw the conclusion that the inclusions

http://dx.doi.org/10.5772/intechopen.70953

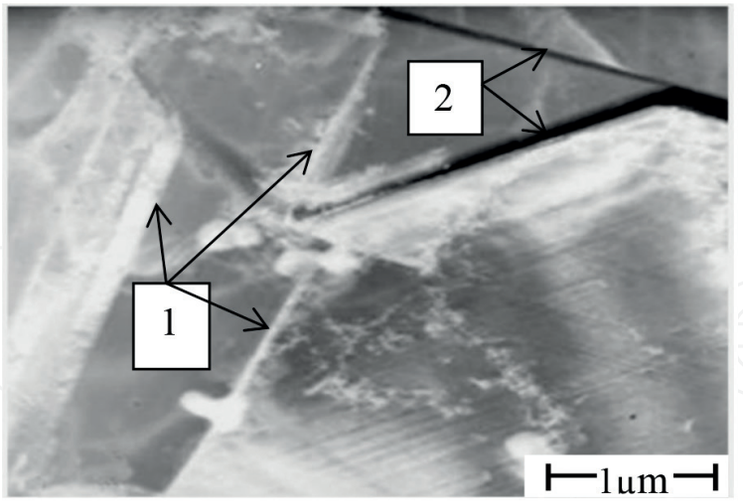

Figure 13. (1) Stacking faults, (2) slip bands and microcracks in a Cr-Ni-Nb austenitic steel.

always initiate the formation of microcracks. The thing is that this process also can depend on factors such as the size of inclusions and the magnitude of elastic stresses before the tip of the microcrack, etc. [9].

6. Discussion

According to the experimental results obtained in the proposed work, a macrocrack is localized within a narrow zone with the width of 600 μm, in which isolated individual mesocracks and slip bands are also observed. To the opinion of the author, the presence of the slip bands in the plastic zone, so that at the initial stage the majority of them are oriented at an angle of 45° to the loading axis and at an angle of 80° after subsequent tests, is not incident. Presumably, when slip takes place at an angle of 45°, at the beginning, it coincides with the direction of maximal tangent stresses. It is obvious to assume that within the plastic zone a local strengthening occurs. After strengthening, another system of slip begins to contribute that coincides or is oriented close to the crack propagation direction. Consequently, the area of maximal deformation shifts to the direction of the main crack. The latter leads to the nucleation of new slip bands, orientated at different angles from the initial ones. This is the evidence of the fact that the slip bands at initial stage of deformation are formed on large microstructure elements. At subsequent deformations slip bands in smaller elements come into action as well [9]. As it was pointed out above, deformation in the plastic zone flows heterogeneously. In addition to the heavily deformed grains, some partially deformed or even non-deformed grains were also observed. In addition, in the locations with no sign of plastic deformation, the isolated microcracks were observed, partly nucleated on (or along) the straight boundaries of grains and microstructure elements of the steel. The distribution and locations of the isolated mesocracks show that the formation of the isolated microcracks is a consequence of stress relaxation. The formation of isolated mesocracks requires at least the following conditions: (1) Grain boundaries should be crystallographic. (2) Slip bands should be oriented parallel to grain boundaries.

(3) Slip should start at grain boundary and then stop. Obviously, the probability of simultaneous implementation of the above conditions is rather small and so is the probability of formation of mesocracks on grain boundaries, especially of their detection. Observation of the isolated mesocracks within the austenite grains (not on the slip bands), in some cases, indicates that the nucleation sites of the isolated mesocracks are the areas of concentration of maximal internal stresses. Thus, during the fatigue tests, demonstration of the following effects is expected: (1) External and internal stresses are summed. (2) External stress facilitates relaxation of internal stresses. Obviously, in the places where the relaxation process is over, the nucleation of microcracks is expected. It is also possible that the relaxation is not finished for some certain reasons; nevertheless, the microcrack is nucleated, but the isolated mesocracks are shorter than the observed slip bands. The latter is obvious from the curve of statistical distribution of the lengths of the isolated mesocracks (**Figures 2–4**). It is clear that there are definite areas and the respective mesocracks with the less length than it was detected in our experiments. It is also difficult because of the simultaneous presence of products of etching, precipitates, grain boundaries, etc. on the polished surface of the sample. Nucleation of the first slip bands on twin and grain boundaries, as well as of the isolated mesocracks, is not a chance. As it is clear from the curves of statistical distribution, the lengths of the slip bands and the microstructure elements are comparable. Therefore, the refinement of grains and the respective microstructure elements of the steel cause the reduction of inhomogeneity of plastic deformation. The number of dislocations in cluster and the amount of accumulated energy are decreasing because the free path of dislocation and consequently the length of slip bands are decreasing. The latter reduces the probability of microcracks' nucleation under the given conditions of fatigue deformation. As it was noted, we observed the macrocracks created after 20–30% of the entire deformation is accomplished. One may conclude that several structural changes occur in the steel just in this period. Finally, some of them contribute to creation of the first microcracks. The deformation flows inhomogeneously as in the plastic zone as well as in the whole sample. From our experiments it follows that in the places of macrocrack deviation, intensive formation of slip bands occurs. As it was shown in the experimental part of the present work, the macrocrack does not preferably passes neither through grain boundaries nor precipitates and does not touch the isolated mesocracks and slip bands as well. Thus, one may suppose that its path, most likely, passes parallel to the elastically stressed microstructural elements of the steel, while the microcrack is nucleated directly in or along the slip bands. It is obvious that when the directions of slip bands are parallel to grain boundaries or to the boundaries of microstructure elements, nucleation of microcracks is simpler. The comparison of the samples undergone to different numbers of cycles but with the same amplitude showed that the increase in frequency directly proportionally decreases the minimal number of cycles leading to the complete destruction. The latter is characteristic to all the investigated steels despite of heat treatment. Hereby, it may be assumed that the fatigue fracture depends on both, the amplitude and the intensity of stress. Accordingly, our investigations showed that fracture in the sample starts with a creation of microcrack. This means that before the formation of mesocrack, several structural changes (slip, twinning) take place in the steel. They initiate creation of martensitic phase and microcracks as well. The microcracks are crystallographically shaped and are nucleated along the slip bands and on grain boundaries, under the favorable circumstances. They are found at a distance of 250–300 μm from the tip of

macrocrack [6]. This fact, once again, indicates that they are of deformation origin and are in close relations with the structural transformations happening in the steel. The revealing of martensite in plastic zone indicates a complexity of mechanism of relaxation of stresses. Apparently, in the beginning, the plastic deformation flows through slip and twinning. However, after strengthening of austenite, martensitic transformation becomes energetically more preferable, or deformation of austenite and martensitic transformation are taking place simultaneously (especially at high values of amplitudes of cyclic deformation)[4]. Consequently, the orientation of micro-cleavages should change while crossing the boundary. The latter is detected experimentally. From our SEM investigations also follow that the macrocrack in steel is created after 20–30% of the entire deformation is accomplished. The latter indicates that at this stage (preliminary), preparatory process takes place in the steel, such as the local and homogeneous slip, creation of dislocation clusters, cells, polygons, etc. Thus, it is generally adopted that mesocracks are formed and propagated on grain and subgrain boundaries. According to our experience, frequently mesocracks and microcracks propagate past subgrain boundaries not touching it. In addition, there are few examples when microcrack passes along the grain or subgrain boundary (**Figures 1**, **2** and **4**). Nevertheless, if the above occurs, such grain or subgrain boundary is strongly linear and even crystallographic, oriented parallel to <110> directions. It is also obvious that in such cases slip bands and dislocation tracks, directions of which are well known for the FCC crystals, are always parallel to the grain boundaries. As what follows from our experimental studies, within 0.5–5.0 hours after preparation of thin foils of the investigated austenitic steel, a redistribution of internal stresses occurs in them. The relaxation and redistribution of stresses occur in homogeneously. In the limits of the examined micro-regions, as was shown above, stacking faults, slip bands, twins, and microcracks are simultaneously observed. Fracture as well as slip, twinning, fragmentation, disorientation, etc. is the relaxation processes, and one of the important reasons of steel fracture is the decrease in their relaxation ability under plastic (dynamic or fatigue) loading. The elastic stresses decrease during fracture, and this leads to the formation of free surfaces. At high stresses, fracture (or microcrack propagation) occurs and is realized after all the above processes are exhausted. However, it does not mean that there is any sequence in the formation of defects. Moreover, some processes at high stresses may flow simultaneously, taking into account the crystallography and Schmidt factor. Thus, the results confirm that ahead of microcrack tip big elastic stresses are concentrated. However, it is quite problematic, and in some cases even impossible, to reveal the field of elastic stresses. In the process of stress relaxation in steels, the dislocations will slide along the crystallographic directions. Therefore, depending on the crystallographic orientation of the thin foil surface, different and nonsymmetric defects will be seen in microscope. Rarely, the archlike extinction contours will also be observed. This means that the observed contour exposes retained elastic stresses existing ahead of microcrack tip. The damaged versions of the proposed model occur in different crystallographic sections (while tilting the specimen), and the scheme projected on the surface of the foil is not always symmetric. As shown in the previous works of the author, the exception is a section through (111) of FCC lattice, taking into consideration the above argumentation. Consequently, determination of plastic zone shape at the tip of a microcrack may be attributed to the theoretical problems (Section 3.4), but for all that, the local crystallography of the material should be taken into account (Section 5). Since slip directions in FCC structures are of

<110> type, with 60° angles between them, and in the BCC of <111> type, with 70° angles between them, the relaxation process in the first case may flow in the six equivalent directions of <110> type, while in the second, just in four directions of <111> type. Taking into account the other ways of relaxation such as twinning in all possible directions, the problem becomes more complicated; in the process of microcrack propagation, the retained stresses are summed; and the relaxation commences through the formation of the above listed defects [10]. On the other hand, the trace analysis and microdiffraction studies inside grain showed that the slip planes are of {111} type and the directions of slip are <110>. The directions of propagation of microcracks are also <110> directions. TEM studies also showed that microcracks are oriented along deformation twins which are crystallographically determined. The microdiffraction, trace, and stereographic analyses of the steel showed that twin plane is a plane of {111} type. The directions of the deformation twins are $<62\bar{4}>$ [130] and $<28\bar{6}>$ [123]. The directions of meso- and microcracks also are the directions of the deformation twins $<62\bar{4}>$ and <286>. It may be supposed from the above that plane of fracture and the plane of twinning {111} coincide in this case. The directions of microcrack propagation coincide with the directions of traces of twinning plane and the slip bands. Therefore, the crystallography of the material plays an important role in fracture process and propagation of micro- and mesocracks. Namely, crystallography of the material determines the location and nucleation process of microcracks [8, 9]. On the scale of the entire microstructure, the changing crystallographic orientations of grains, naturally, can create inhomogeneous stress fields. The magnitudes of such fields and their influence, on the processes of crack formation, could not be taken into account in the mechanical characteristics upon testing to failure. However, as our studies showed, in the case of small cracks, especially on micro- and nano-level, the local anisotropy cannot be neglected. The formation of slip bands obeys the crystallography of the material. Microcracks are initiated in slip bands and grow along them. The formation and propagation of microcracks are also governed by the crystallography and local anisotropy of micro-regions and the entire grains. Therefore, as a microcrack grows, its shape and trajectory will always depend on the anisotropy of the grains through which it propagates. To this factor, a not uniform distribution of stresses in the bulk of the sample is also added. All this will of course affect the trajectory of the microcrack, in any case, during its growth to meso-dimensions.

7. Conclusions

1. The macrocrack in steel is formed only after 20–30% of the total deformation, and the deformation process in the sample flows inhomogeneously.
2. In the zone of destruction, a martensitic phase is formed, and its volume fraction is directly proportional to the amplitude and frequency of cyclic deformation.
3. The trace, stereographic analysis, and microdiffraction studies proved that the directions of microcracks, slip bands, and deformation twins coincide. The trajectory of microcrack and plane of fracture, within an austenite grain, are governed by the crystallography of the material. A fracture plane is a plane of {111} type and a propagation direction (<110>).

4. The formation of microcracks in slip bands is a consequence of local plastic deformation, whose energy advantageousness is ensured by the relaxation of peak stresses and by the reserve of energy in dislocation cores.
5. Sometimes, inclusions can become barriers for the propagation of microcracks.
6. The study of the interaction of microcracks, with each other, showed that their coalescence or stopping depends on the angle of their joining and on the internal stresses accumulated in the plastic zone ahead of the tips of the microcracks.

Acknowledgements

The research was supported by the ISTC grant G-719, for what the authors are grateful to the Japanese Government, by Shota Rustaveli National Science Foundation, P/N GNSF/ST06/7-072, and by the Georgian Technical University for financing the chapter.

Author details

Tamaz Eterashvili

Address all correspondence to: tetrcsu@gtu.ge

Republic Center for Structure Researches, Georgian Technical University, Tbilisi, Georgia

References

[1] Chang MS, Ritchie RO, Kang YG. Growth behavior of short surface fatigue cracks in 2 1/4 Cr-1 Mo steel. KSME Journal. September 1989;**3**(2):78-85. DOI: 10.1007/BF02953592

[2] Roberts SG. Modeling crack tip plastic zones and brittle-ductile transition. Materials Science and Engineering A. 1997;**234-236**:52-58. DOI: 10.1016/S0921-5093(97)00180-9

[3] Ravichandran KS, Li X. D, Fracture Mechanics. Character of Small Cracks in Polycrystalline Materials: Concept and Numerical K Calculations. Acta Materialia. 2000; **48**:525-540. DOI: 10.1016/S1359-6454(99)00348-1

[4] Eterashvili T, Dzigrashvili T. Study of fracture mechanisms at cyclic fatigue of steels used in nuclear reactors I. Steel Research International. 2012;**83**(3):213-217. DOI: 10.1002/srin.201100184

[5] James R. Dislocation nucleation from a crack tip: An analysis based on the Payer's concept. Journal of the Mechanics and Physics of Solids. 1992;**40**(2):239-271. DOI: doi.org/10.1016/S0022-5096 (05)80012-2

[6] Eterashvili TV. Study of fatigue processes occurring in the plastic zone in front of the tip of a microcrack in austenitic steels (I). Fizika Metallov i Metallovedenie. 2006;**101**(2):200-205. DOI: 10.1134/S0031918X06020128

[7] Eterashvili T. Electron-microscopic study of the formation and distribution of microcracks in austenitic steels upon low-cycle fatigue tests. Fizika Metallov i Metallovedenie. 2010;**110**(6):624-627. DOI: 10.1134/S0031918X10120112

[8] Eterashvili T, Vardosanidze M. A fracture crystallography and anisotropy of propagation of microcracks nucleated in stainless austenitic steels after LCF. Key Engineering Materials. 2006;**324-325**:935-938. DOI: 10.4028/www.scientific.net/KEM.324-325.935

[9] Eterashvili T, Dzigrashvili T, Vardosanidze M. Deviations of microcrack during propagation in thin films of austenitic steel and accompanying accommodative processes. Key Engineering Materials. 2015;**627**:297-300, 796. DOI: 10.4028/www.scientific.net/KEM.627.297

[10] Eterashvili T, Dzigrashvili T, Vardosanidze M. The analysis of microcrack tip plastic zone formed in thin films after LCF tests of austenitic steel used in NPP I. Key Engineering Materials. 2010;**417-418**:109-112. DOI: 10.4028/www.scientific.net/KEM.417-418.10